

Nuclear stability and the Fold Catastrophe

Samyak Jain

ORCID: 0009-0000-7455-782X

Department of Physics, Indian Institute of Technology Bombay, Powai, Mumbai 400 076, India*

A. Bhagwat

ORCID: 0000-0002-3479-1301†

School of Physical Sciences, UM-DAE Centre for Excellence in Basic Sciences,
University of Mumbai, Kalina Campus, Mumbai 400 098, India

(Dated: November 27, 2023)

A geometrical analysis of the stability of nuclei against deformations is presented. In particular, we use Catastrophe Theory to illustrate discontinuous changes in the behavior of nuclei with respect to deformations as one moves in the $N - Z$ space. A third-order phase transition is found in the liquid-drop model, which translates to a complete loss of stability (using the Fold catastrophe) when shell effects are included. The analysis is found to explain the instability of known fissile nuclei and also justify known decay chains of heavy nuclei.

I. INTRODUCTION

Developed in the 1970s by René Thom, Catastrophe theory[1] is a geometrical framework that explains discontinuous changes in dynamical systems. Thom showed that any function of $r \leq 5$ parameters can be mapped to one (and only one) of 11 known families of functions (catastrophes). One can thus study a wide range of systems by mapping their potential to one of these catastrophes. These catastrophes have been well-studied for discontinuous features, which can be mapped back to the system of interest to find where these changes occur. The proof of the theorem can be found in [2] and [3]; we shall take it as a given.

The theory's application to quantum systems is trickier since one must use semi-classical methods to write a classical version of the quantum Hamiltonian. In particular, nuclei present a suitable testing ground for this since nuclear decays (especially fission) are well-studied discontinuous phenomena that would provide experimental verification for any analysis conducted. In this work, we consider the liquid-drop model and the shell model. In Section II, we outline the generalization of the liquid-drop model to deformed shapes as presented in [4]. In Section III, we then discuss the stability analysis of the model and find a third-order phase transition. In Section IV, we outline the shell model as presented in [4], and how it is incorporated into the liquid-drop model as a correction term. In Section V, we map the final deformation energy to the fold catastrophe and find a complete loss of stability as one moves in the $N - Z$ space, and see how this explains observed fissile nuclei and decay chains of heavy nuclei in Section VI.

II. THE DEFORMED LIQUID DROP MODEL

We begin with the spherical liquid-drop model as presented in [4]:

$$B = a_v A [1 - k_v I^2] - a_s A^{2/3} [1 - k_s I^2] - a_C \frac{Z^2}{A^{1/3}} \quad (1)$$

where B is the binding energy of the nucleus, a_v, a_s, a_C, k_v and k_s are constants, Z is the atomic number, N is the neutron number and

$$I = \frac{N - Z}{N + Z} \quad (2)$$

The values of the constants are obtained through best fits and have been stated in [4] and [5] as

$$a_C = 0.7053, \quad a_s = 17.944 \text{ MeV}, \quad k_s = 1.782 \quad (3)$$

The parameter k_v is in the range 1.5 - 2.0 [4], however, the parameter is not relevant in the analysis reported here.

The model has a volume term (proportional to the volume), a surface term (proportional to the surface area), and a coulomb term respectively. This model can be generalized to a deformed nucleus by simply accounting for the change in the surface area and coulomb interactions and rewriting B as

$$B = a_s A^{2/3} (1 - k_s I^2) \frac{E_s(d)}{E_s^0} + a_C \frac{Z^2}{A^{1/3}} \frac{E_C(d)}{E_C^0} \quad (4)$$

where we assume that any deformations conserve the volume of the nucleus, making the volume term irrelevant. $E_C(d), E_s(d)$ are the surface and coulomb energies of the deformed nucleus, and E_s^0, E_C^0 are the surface and coulomb energies of the spherical nucleus

$$E_s^0 = a_s A^{2/3} (1 - k_s I^2) \quad (5)$$

$$E_C^0 = a_C \frac{Z^2}{A^{1/3}} \quad (6)$$

* Corresponding author: samyakjain02@gmail.com

† Contributing author: ameeya@cbs.ac.in

The shape of a deformed nucleus can be parameterised using spherical harmonics as

$$R(\theta, \phi) = R_\alpha \left[1 + \sum_{\lambda=1}^{\infty} \sum_{\mu=-\lambda}^{\lambda} \alpha_{\lambda\mu} Y_{\lambda\mu}(\theta, \phi) \right] \quad (7)$$

To simplify this, we assume that the deformations of the nucleus are symmetric about an axis (taken to be the z axis). Thus, we can work with Legendre Polynomials instead of spherical harmonics; we only need to consider $\mu = 0$ in the summation. We define $\beta_\lambda = \alpha_{\lambda\mu}$ and use

$$Y_{\lambda 0}(\theta, \phi) = \left(\frac{2\lambda + 1}{4\pi} \right)^{1/2} P_\lambda(\cos(\theta)) \quad (8)$$

We thus obtain

$$R(\theta) = R_\beta \left[1 + \left(\frac{2\lambda + 1}{4\pi} \right)^{1/2} \sum_{\lambda=1}^{\infty} \beta_\lambda P_\lambda(\theta) \right] \quad (9)$$

It turns out only β_2 (up to its third power) is relevant for small deformations ([4]). As shown in [4], the Coulomb and the surface energies for small deformations can be calculated as

$$E_C = E_C^0 \left(1 - \frac{1}{5} a_2^2 - \frac{4}{105} a_2^3 \right) \quad (10)$$

$$E_s = E_s^0 \left(1 + \frac{2}{5} a_2^2 - \frac{4}{105} a_2^3 \right) \quad (11)$$

where

$$a_2 = \sqrt{\frac{5}{4\pi}} \beta_2 \quad (12)$$

Thus, the additional energy due to deformations is

$$\Delta E = (E_s + E_C) - (E_s^0 + E_C^0)$$

giving us

$$\Delta E = V_d = E_s^0 \left(\frac{2}{5} (1 - x) a_2^2 - \frac{4}{105} (1 + 2x) a_2^3 \right) \quad (13)$$

where

$$x = \frac{E_C^0}{2E_s^0} = \frac{a_C Z^2}{a_s A} \frac{1}{1 - k_s I^2} \quad (14)$$

x is the so-called fissility parameter; as [4] shows, it is a measure of how easy it is for a nucleus to undergo fission. We plot x as a function of N for $Z = 92$ in Fig.1.

We now examine the deformation energy V_d (Eq. 13) for instabilities and phase transitions.

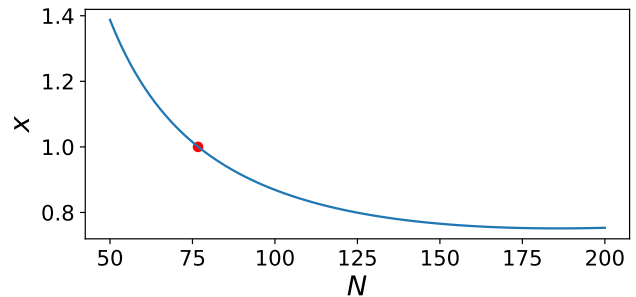


FIG. 1: x as a function of N for $Z = 92$. The point at which $x = 1$ is marked.

III. THE THIRD-ORDER PHASE TRANSITION

We note that both x and E_s^0 are functions of Z and N . Let us consider a fixed Z , for which we slowly vary N from smaller to larger values. Since Z is constant, we can say that x and E_s are functions of N . We consider N to be a parameter, and treat a_2 as a coordinate. We assume that the ground state of the system dwells at the lowest energy minimum. We study how the system's energy (the energy the lowest energy minimum) varies with N .

We have

$$V_d(N) = E_s^0(N) \left(a(N) a_2^3 + b(N) a_2^2 \right) \quad (15)$$

where

$$\begin{aligned} a(N) &= -\frac{4}{105} (1 + 2x(N)) \\ b(N) &= \frac{2}{5} (1 - x(N)) \end{aligned} \quad (16)$$

It can be easily shown from Eq.(5) that $E_s(N)$ is a smooth and positive function of N in the region of interest. Further, $a(N) < 0$ for all $N > 0$.

The fixed points of the system a_2^0 are given by

$$\frac{\partial V_d}{\partial a_2} = 0 \Rightarrow a_2^0 = 0, -\frac{2b}{3a} \quad (17)$$

Further

$$\begin{aligned} \frac{\partial^2 V}{\partial a_2^2}(0) &= 2b \\ \frac{\partial^2 V}{\partial a_2^2}\left(-\frac{2b}{3a}\right) &= -2b \end{aligned} \quad (18)$$

For $b > 0$ the equilibrium at $a_2 = 0$ is stable and the equilibrium at $a_2 = -\frac{2b}{3a}$ is unstable. For $b < 0$, the equilibrium at $a_2 = 0$ is unstable and the equilibrium at $a_2 = -\frac{2b}{3a}$ is stable.

Thus, at $b = 0$, the fixed points meet, and the stability of the two fixed points swap. For $b > 0$ the system dwells at $a_2^0 = 0$. The energy of the system is

$$V_d(N, a_2^0 = 0) = 0 \quad (19)$$

This is completely independent of N . Thus

$$b > 0 \Rightarrow \frac{d^n V_d(a_2^0 = 0)}{dN^n} = 0 \quad \forall n \in \mathbb{N} \quad (20)$$

Now, for $b < 0$, the system dwells at $a_2^0 = -\frac{2b}{3a}$. The energy of the system is given by

$$V_d \left(N, a_2^0 = -\frac{2b}{3a} \right) = \frac{4b^3}{27a^2} E_s^0 \quad (21)$$

We now evaluate the derivatives of this energy with respect to N , at $b = 0$. We note that a, b, E_s^0 and their derivatives with respect to N are smooth in our region of interest (where most observed nuclei are found in the $N - Z$ space). Also, as noted earlier, $a(N) < 0 \quad \forall N$.

On computing the derivatives, one obtains multiple terms containing derivatives of a, b, E_s^0 . However, since we are evaluating these derivatives at $b = 0$, most of these terms vanish. Using this, one finds easily that, at $b = 0$

$$\frac{dV_d(a_2^0)}{dN} = \frac{d^2 V_d(a_2^0)}{dN^2} = 0 \quad (22)$$

However

$$\frac{d^3 V_d(a_2^0)}{dN^3} = \left(\frac{8}{9} \frac{E_s^0}{27a^2} \left(\frac{db}{dN} \right)^3 \right) \Big|_{b=0} \neq 0 \quad (23)$$

One can verify that x is a decreasing function of N (for a fixed Z) in the region of interest (see Fig.1). From Eq.(16), we see that we cross $b = 0$ at $x = 1$. As N is increased from lower to larger values, x keeps decreasing, and at some $N = N_0$, x falls below 1. Before this point, $b < 0$, and the system's lowest minimum is always given by $a_2^0 = -\frac{2b}{3a}$ (note this is a function of N). The first three derivatives of this energy are given by Eq.(22) and Eq.(23).

At $x = 1$, this minimum stops changing with N and remains fixed at $a_2^0 = 0$. Now, all the derivatives of the system's energy turn to 0. From Eq.(22) and Eq.(23), we see that the first two derivatives are continuous, while the third derivative is discontinuous, implying a third-order phase transition.

One can find the $N = N_0$ at which this phase transition occurs using

$$x(N_0) = 1 = \frac{a_C}{a_s} \frac{Z^2}{A} \frac{1}{1 - k_s I^2} \quad (24)$$

As per this analysis, as one varies N from lower to higher values (for a fixed Z), the nucleus simply goes from preferring a deformed shape to a spherical shape via a third-order phase transition. This in itself does not imply a catastrophic instability one would imagine is needed for fission. We thus now consider a more microscopic nuclear model: the shell model.

IV. THE SHELL MODEL AND SHELL CORRECTION

The liquid-drop model has had success in describing the 'average' behavior of nuclei but fails to account for the existence of magic numbers (neutron and proton numbers for which a nucleus is unusually stable). This extra stability can naturally be attributed to the filling of energy levels.

One considers each nucleon to be in an attractive potential caused by all the other nucleons. A typical choice of this potential (for an undeformed nucleus) is the modified-harmonic oscillator potential given by Nilsson ([6] and [4])

$$V_{\text{MO}}(r) = \frac{1}{2} m \omega_0^2 r^2 - \kappa \hbar \omega_0 (2\mathbf{l} \cdot \mathbf{s} + \mu(l^2 - \langle l^2 \rangle_{\mathcal{N}})) \quad (25)$$

where $\mathcal{N} = 2n + l$ is the principal quantum number. To account for Coulombic interactions and the Pauli exclusion principle, neutrons and protons are considered to experience separate potentials with different natural frequencies ([4])

$$\hbar \omega_0^{N,Z} = 41A^{-\frac{1}{3}} \left(1 \pm \frac{1}{3} \frac{N - Z}{A} \right) \quad (26)$$

The energy levels for the modified harmonic oscillator potential are analytically obtained as ([4])

$$E_{\mathcal{N}l s} = \hbar \omega_0 \left(\mathcal{N} + \frac{3}{2} - \kappa \left[2s \left(l + \frac{1}{2} \right) - \frac{1}{2} \right] - \mu' \left[l(l+1) - \frac{\mathcal{N}(\mathcal{N}+3)}{2} \right] \right) \quad (27)$$

To account for deformations, one simply considers deformations to the spherical potential ([7] and [4]):

$$V = \frac{1}{2} m \omega^2(\varepsilon) r^2 \left(1 - \frac{2}{3} \varepsilon P_2(\cos \theta_t) + \sum_{\lambda=3,4,\dots} \varepsilon_\lambda P_\lambda(\cos \theta_t) \right) \quad (28)$$

Here, the frequency is considered as a function of the deformations to account for the volume conservation of an equipotential surface, and the factor of $2/3$ allows for simpler calculations later. One can find the shifts in the energy levels due to the deformations using perturbation theory. Let these energy levels be $e_\nu(\varepsilon)$ (where ν iterates over each nucleon, not each energy level, so degenerate energy levels are counted multiple times). To obtain the total energy of the nucleus, one can't simply add up the individual nucleon energies because of overcounting of inter-nucleon interactions. Since the liquid-drop model accounts well for the average behavior of nuclei, one incorporates the shell effects as a correction to the liquid-drop model.

This correction procedure is described in [4]: since the ‘average’ behavior of nuclei is reproduced well by the liquid-drop model, one adds the shell model’s deformation energy to the liquid-drop model and subtracts an ‘averaged’ shell model energy (so that the new corrected energy still describes the average behavior of nuclei correctly).

To compute this ‘averaged’ shell model energy, consider the shell model’s energy density

$$g(e) = \frac{1}{\gamma} \sum_{\nu} \delta(\xi_{\nu}) \quad (29)$$

where γ is an energy scale to make the argument of the Dirac-delta dimensionless, and $\xi_{\nu} = \frac{e - e_{\nu}}{\gamma}$. The total energy is then

$$E = \int eg(e)de = \sum_{\nu} e_{\nu} \quad (30)$$

irrespective of γ . To obtain an averaged energy density, one smears the energy levels by expanding out the Dirac-delta functions in a Hermite polynomial expansion

$$\delta(x) = \sum_{n=0}^{\infty} \frac{1}{\sqrt{\pi}} c_n e^{-x^2} H_{2n}(x) \quad (31)$$

where

$$c_k = \frac{(-1)^k}{(2k)!! 2^k} \quad (32)$$

and truncating this expansion at some order n to obtain

$$\tilde{g}(e) = \frac{1}{\gamma\sqrt{\pi}} \sum_{\nu} \sum_{k=0}^n c_k e^{-\xi_{\nu}^2} H_{2k}(\xi_{\nu}) \quad (33)$$

Then, γ decides the scale of this smearing, and is typically chosen as $\hbar\omega_0$. One chooses an n so that the resulting energies are relatively independent of γ , and [4] shows this is observed at $n = 3$.

The difference of these energy densities is then

$$g(e) - \tilde{g}(e) = \frac{1}{\gamma\sqrt{\pi}} \sum_{\nu} \sum_{k=n+1}^{\infty} c_k e^{-\xi_{\nu}^2} H_{2k}(\xi_{\nu}) \quad (34)$$

Then, as per the correction outlined earlier, the total energy is

$$\begin{aligned} E &= E_{LD} + E_{corr} \\ &= E_{LD} + \sum_{\nu} \sum_{k=n+1}^{\infty} \int \frac{e c_k}{\gamma\sqrt{\pi}} e^{-\xi_{\nu}^2} H_{2k}(\xi_{\nu}) de \end{aligned} \quad (35)$$

where E_{LD} is the liquid-drop energy. To find the energy due to deformation, we simply need to include the deformation dependence of the energy levels

$$V(\vec{\varepsilon}) = V_d(a_2) + \sum_{\nu} \left. \frac{\partial E_{corr}}{\partial e_{\nu}} \right|_{\vec{\varepsilon}=0} \Delta e_{\nu} \quad (36)$$

where $V_d(a_2)$ is given by Eq.(15). We shall later link the deformation parameters ε and a_2 .

V. STABILITY ANALYSIS

Since the shell model is being incorporated with the liquid-drop model, we consider only ε in the expansion given by Eq.(28):

$$V = \frac{1}{2} m\omega^2(\vec{\varepsilon}) r^2 \left(1 - \frac{2}{3} \varepsilon P_2(\cos \theta_t) \right) \quad (37)$$

We can then write the perturbed (deformed) Hamiltonian as

$$H = H_0 + \varepsilon H' \quad (38)$$

where

$$H' = -\frac{2}{3} m\omega_0^2 r^2 P_2(\cos \theta) \quad (39)$$

The shifts in energy levels are then computed in [4] as

$$\Delta E = \langle \varepsilon H' \rangle = \frac{1}{6} \varepsilon m\omega(\varepsilon)^2 \langle r^2 \rangle \frac{3m_j^2 - j(j+1)}{j(j+1)} \quad (40)$$

where $j = l + s$ and a $2j + 1$ degeneracy is broken. Considering the timescales of the deformations are small enough, we assume that upon deformation, a nucleon will pick the m_j which minimizes the change in energy with respect to its energy before the deformation. We see that ΔE is minimized for $m_j = \pm j$. Thus, the energy shift for deformed energy levels is given by

$$\Delta E = \langle \varepsilon H' \rangle = \frac{1}{6} \varepsilon m\omega(\varepsilon)^2 \langle r^2 \rangle \frac{2j-1}{(j+1)} \quad (41)$$

To obtain $\omega(\varepsilon)$ in Eq.(28), volume conservation of the equipotential surface

$$\omega(\varepsilon) = \omega_0 \left(1 + \frac{1}{9} \varepsilon^2 \dots \right) \quad (42)$$

Plugging Eq.(42) and Eq.(41) in Eq.(36), we obtain (up to third order in ε)

$$V(\vec{\varepsilon}) = V_d(\vec{\varepsilon}) + c(N, Z) \left(\varepsilon + \frac{2\varepsilon^3}{9} \right) \quad (43)$$

where $c(N, Z)$ incorporates all the proportionality coefficients and is given by

$$c(N, Z) = \sum_{\nu} \frac{1}{6} m\omega_0^2 \langle r^2 \rangle \frac{2j-1}{j+1} \left. \frac{\partial E_{corr}}{\partial e_{\nu}} \right|_{\varepsilon=0} \quad (44)$$

One can easily calculate $\langle r^2 \rangle$ to be ([4])

$$\langle r^2 \rangle = \left(\mathcal{N} + \frac{3}{2} \right) \frac{\hbar}{m\omega_0} \quad (45)$$

leading to

$$c(N, Z) = \sum_{\nu} \frac{1}{6} \hbar\omega_0 \left(\mathcal{N} + \frac{3}{2} \right) \frac{2j-1}{j+1} \left. \frac{\partial E_{corr}}{\partial e_{\nu}} \right|_{\varepsilon=0} \quad (46)$$

To link the deformation ε with the deformation a_2 considered in the liquid-drop model, we simply consider an equipotential surface for the deformed potential (Eq.(37))

$$r(\theta) = r_0 \left(1 + \frac{2\varepsilon}{3} P_2(\cos\theta) \right) \quad (47)$$

Comparing this to the spatial deformations considered in the liquid-drop model (Eq.(9), we immediately see

$$\varepsilon = \frac{3}{2} \sqrt{\frac{5}{4\pi}} \beta_2 = \frac{3}{2} a_2 \quad (48)$$

Substituting this and $V_d(a_2)$ in Eq.(43), we obtain

$$V(a_2) = Aa_2^3 + Ba_2^2 + Ca_2 \quad (49)$$

where

$$A = E_s^0(N)a(N, Z) + \frac{3c(N, Z)}{4}$$

$$B = E_s^0(N, Z)b(N, Z)$$

$$C = \frac{3}{2}c(N, Z) \quad (50)$$

We now appeal to Catastrophe theory. An obvious choice of a catastrophe to map $V(a_2)$ is the fold catastrophe:

$$V_t(u) = u^3 + tu \quad (51)$$

where t is a parameter and u is a coordinate. Notably, the fold catastrophe has a pitchfork bifurcation at $t = 0$. For $t < 0$, the potential has a maximum and a minimum, which meet and annihilate at $t = 0$. For $t > 0$, no stable point exists in the system, leading to a drastic change in the system's behavior.

One can easily check that $Ax^3 + Bx^2 + Cx$ can be mapped to $u^3 + tu + s$ via the mapping

$$x = \frac{u}{A^{1/3}} + p \quad (52)$$

where

$$p = \frac{-B}{3A}, \quad t = \frac{3AC - B^2}{3A^{4/3}}, \quad s = \frac{2B^3 - 9ABC}{27A^2} \quad (53)$$

Here, s is an additive term with no coordinate dependence and can be safely discarded. Under this mapping, one observes the loss of stability at $t > 0$, which translates to

$$t > 0 \Rightarrow \frac{3AC - B^2}{A^{4/3}} > 0 \quad (54)$$

Defining this expression as $f(N, Z)$, we get

$$f(N, Z) = \left[E_s^0(N)a(N, Z) + \frac{3}{4}c(N, Z) \right]^{-4/3} \times$$

$$\left(\frac{9}{2} \left[\frac{3}{4}c(N, Z) + E_s^0(N)a(N, Z) \right] c(N, Z) \right.$$

$$\left. - \left[E_s^0(N, Z)b(N, Z) \right]^2 \right) > 0 \quad (55)$$

VI. EXPERIMENTAL VERIFICATION

To compare with observables, we plot $f(N, Z)$ in the $N - Z$ space. The values of the shell model parameters κ and μ for various \mathcal{N} levels are shown in Table I ([4]).

$c(N, Z)$ is symbolically evaluated in python. We plot $f(N, Z)$ as a heat map in the $N - Z$ space, leading to Fig.(2). We observe a band-like structure, with nuclei in

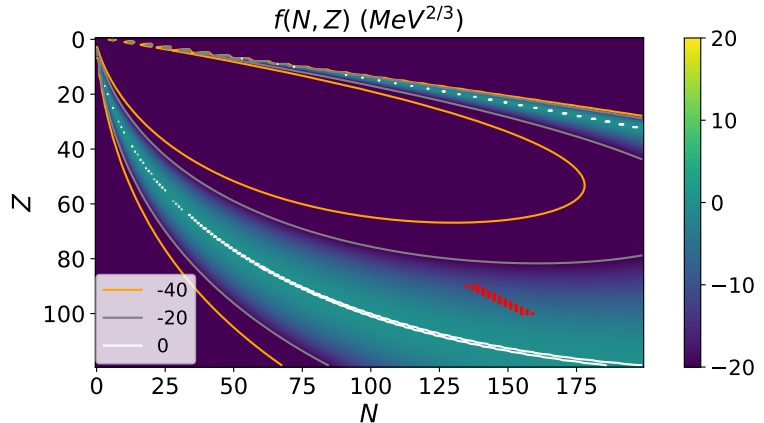


FIG. 2: $f(N, Z)$ is plotted in the $N - Z$ plane. A band-like structure is seen in which $f(N, Z)$ is positive or close to 0, indicating a loss of stability. Various contours are added, and nuclei satisfying Ronen's fissile rule are scattered in red. The contour of $f(N, Z) = 0$ is marked in white; these nuclei favor spontaneous deformations from a spherical shape.

the interior of the band having $f(N, Z) < 0$ and being stable and those near the periphery having higher values of $f(N, Z)$. We note here that any nuclei with a positive $f(N, Z)$ are inherently unstable, and we would not expect to see them at all. Instead, we can use $f(N, Z)$ as a measure of how unstable a nucleus is, with higher values implying less stability. We also add some contours and mark nuclei satisfying Ronen's fissile rule ([8]): nuclei satisfying

$$90 \leq Z \leq 100, \quad 2Z - N = 43 \pm 2 \quad (56)$$

are fissile. We see that all the nuclei lie close to the band periphery, where there is a sudden sharp increase in $f(N, Z)$ (implying a sudden increase in instability). Another test is to see how $f(N, Z)$ varies across decay chains. We show this for various decay chains in Fig.3.

TABLE I: μ and κ values for various $\mathcal{N} = 2n + l + 1$ levels

$\mathcal{N} = 2n + l + 1$	μ	κ
2	0	0.8
3	0.0263	0.075
4,5,6,7	0.024	0.06

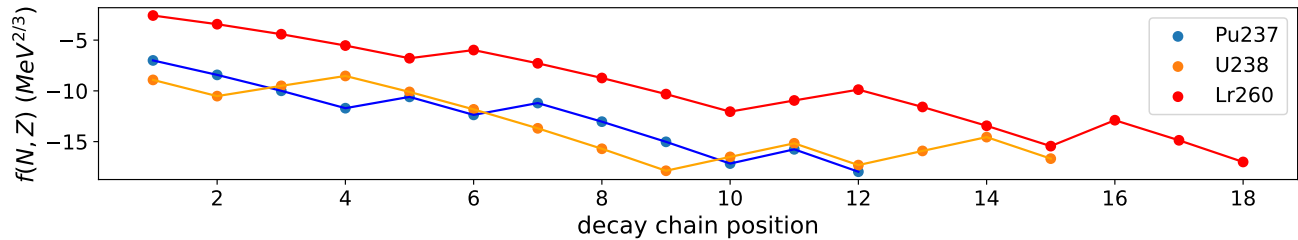


FIG. 3: Evolution of $f(N, Z)$ in various decay chains is shown. Note the jumps at each β decay. Decay chains:

- 1) $U238 \xrightarrow{\alpha} Th234 \xrightarrow{\beta} Pa234 \xrightarrow{\beta} U234 \xrightarrow{\alpha} Th230 \xrightarrow{\alpha} Ra226 \xrightarrow{\alpha} Rn222 \xrightarrow{\alpha} Po218 \xrightarrow{\alpha} Pb214 \xrightarrow{\beta} Bi214 \xrightarrow{\beta} Po214$
 $\xrightarrow{\alpha} Pb210 \xrightarrow{\beta} Bi210 \xrightarrow{\beta} Po210 \xrightarrow{\alpha} Pb206$
- 2) $Pu237 \xrightarrow{\alpha} U233 \xrightarrow{\alpha} Th229 \xrightarrow{\alpha} Ra225 \xrightarrow{\beta} Ac225 \xrightarrow{\alpha} Fr221 \xrightarrow{\beta} Ra221 \xrightarrow{\alpha} Rn217 \xrightarrow{\alpha} Po213, Pb209 \xrightarrow{\beta} Bi209 \xrightarrow{\alpha} Tl205$
- 3) $Lr260 \xrightarrow{\alpha} Md256 \xrightarrow{\alpha} Es252 \xrightarrow{\alpha} Bk248 \xrightarrow{\alpha} Am244 \xrightarrow{\beta} Cm244 \xrightarrow{\alpha} Pu240 \xrightarrow{\alpha} U236 \xrightarrow{\alpha} Th232 \xrightarrow{\alpha} Ra228 \xrightarrow{\beta} Ac228 \xrightarrow{\beta} Th228$
 $\xrightarrow{\alpha} Ra224 \xrightarrow{\alpha} Rn220 \xrightarrow{\alpha} Po216 \xrightarrow{2\beta} Rn216 \xrightarrow{\alpha} Po212 \xrightarrow{\alpha} Pb208$

We observe a drop in $f(N, Z)$ (implying increase in stability) as each decay progresses, consistent with our analysis. Notably, all α decays are seen to decrease $f(N, Z)$. However, we observe that each β decay increases $f(N, Z)$, with a drop again in consequent α decays. Understanding this feature requires further investigation, but this naturally paints a picture of a β decay being an ‘intermediate’ step that allows the decay chain to end at a more stable nucleus (as compared to the one it would have ended at without a β decay) at the expense of some temporary instability in the form of an increase in $f(N, Z)$. This is analogous to a path optimization process; one accepts potentially destabilizing solutions in order to better search for a global optimum solution.

VII. CONCLUSION

We have presented a geometric analysis of the stability of nuclei against deformations using Catastrophe theory. We find a third-order phase transition in the liquid-drop model, in which the nucleus simply goes from preferring a spherical shape to preferring a deformed shape with no characteristic loss of stability. Upon incorporating shell effects, this translates from a phase transition to a complete loss of stability characteristic of the Fold catastrophe. Experimentally, our analysis is seen to explain the instability of fissile nuclei and also explain various decay chains of heavy nuclei, especially α decays. Exploring the optimization picture hinted at by Fig.3 should be a major focus of future work.

VIII. ACKNOWLEDGEMENTS

We would like to thank Vikram Rentala and Kumar Rao for their valuable insights.

-
- [1] R. Thom. *Stabilite Structurelle et Morphogenese*. Benjamin, New York, 1972.
 - [2] T. Poston and I. Stewart. *Catastrophe Theory and its Applications*. Surveys and Reference Works in Mathematics, 1978.
 - [3] V. I. Arnold. *Catastrophe Theory*. Springer Berlin, Heidelberg, 2012.
 - [4] Ingemar Ragnarsson and Sven Gvsta Nilsson. *Shapes and Shells in Nuclear Structure*. Cambridge University Press, 1995.
 - [5] William D. Myers and Wladyslaw J. Swiatecki. Nuclear masses and deformations. *Nuclear Physics*, 81(1):1–60, 1966.
 - [6] S. G. Nilsson. Binding states of individual nucleons in strongly deformed nuclei. *Kong. Dan. Vid. Sel. Mat. Fys. Med.*, 29N16:1–69, 1955.
 - [7] Nilsson et al. On the nuclear structure and stability of heavy and superheavy elements. *Nuclear Physics A*, 1969.
 - [8] Yigal Ronen. A rule for determining fissile isotopes. *Nuclear Science and Engineering*, 152(3):334–335, 2006.